## Supplementary figures and legends.

**Figure S1. (A)** Triglycerides measured by enzymatic methods or by flow cytometry with Nile red and BODIPY 493/503 in Non-loaded, Loaded and Loaded cells treated with TriacsinC 10µM (Loaded+TRC). Values are referred to Non-loaded cells. **(B)** Heterogeneity in LD content in Non-loaded and cells Loaded with 175µg/ml FA from different cell lines. Red bars correspond to hepatic cell lines. Data represent mean ± SEM of 3 independent experiments.

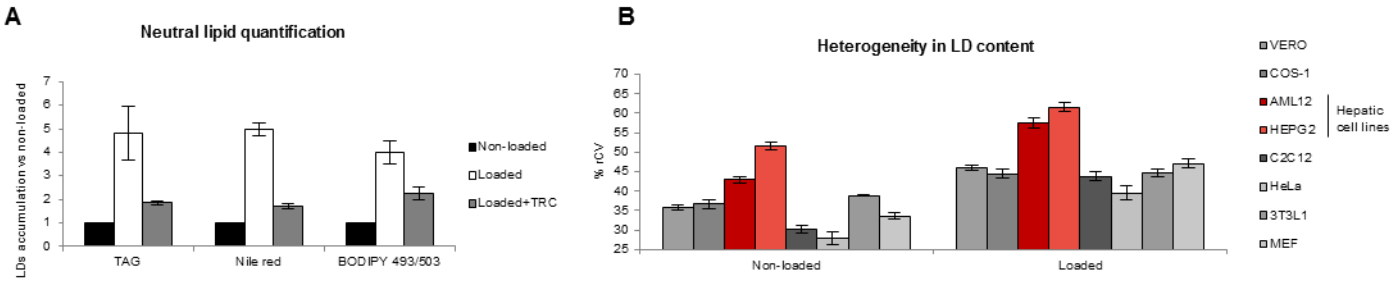


**Figure S2. (A and B)** LD accumulation (A) and heterogeneity (B) of non-loaded cells, loaded cells, and cells additionally loaded with 500µM DEUP, 181µM E600, or 4µM platensimycin (PTM).Statistical significance was calculated versus loaded cells (red bars). **(C and D)** LD accumulation (C) and heterogeneity (D) of non-loaded cells, loaded cells, and cells additionally unloaded 16h in a FA-free medium or in a FA-free medium with 500µM DEUP or 181µM E600. Statistical significance was calculated versus unloaded cells (white bars). **(E and F)** LD accumulation (E) and heterogeneity (F) of asynchronous loaded cells (red bars) and cells synchronized at G0 with 24h of serum starvation (dark grey bars) or at the S phase with 24h 2.5 mM thymidine (THY) treatment (light grey bars) during the 24h of FA loading. **(G)** Representative histograms of the cell cycle profile of cells treated as in E and F and stained for DNA content with Hoechst. Data represent mean ± SEM of at least 3 independent experiments.

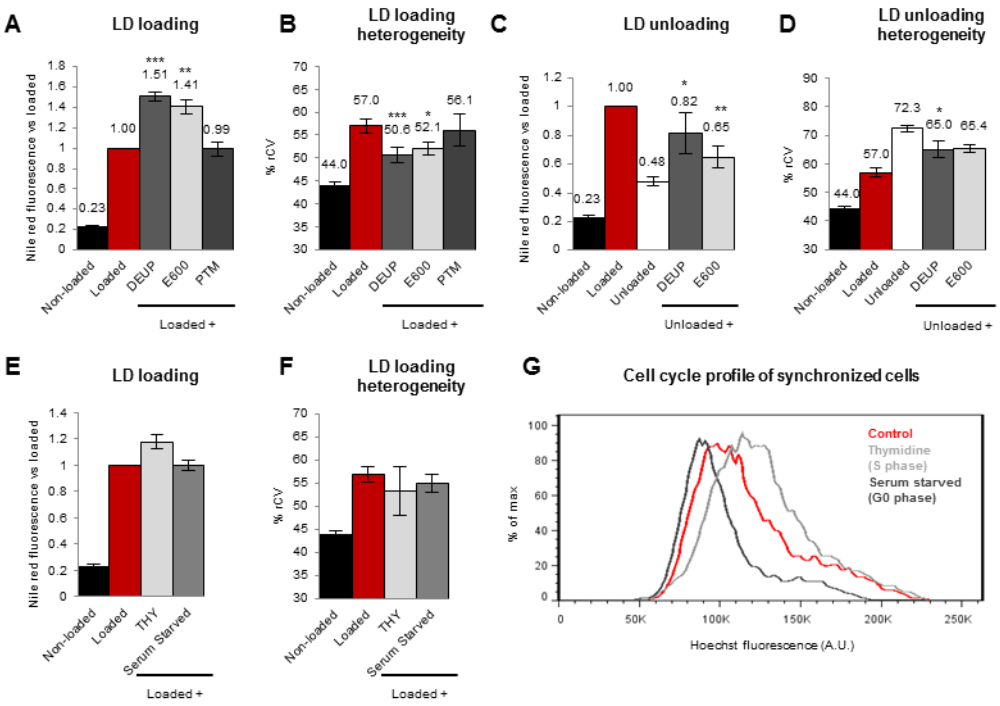


**Figure S3. (A)** FA uptake by high- or low-lipid sorted cells (as in Fig.3) measured as BODIPY-FA fluorescence versus Low-lipid content cells. **(B, left)** Representative dot plot of the SSC-A (LDs) versus BODIPY-FA fluorescence in the whole population of cells divided in Low (40.2% of the population), Medium (43.6% of the population) and High LD content (15.5% of the population). **(B, right)** Mean BODIPY-FA fluorescence corresponding to each selected region versus the mean of the entire population. Statistical significances were calculated versus low-lipid cells (black bars). Data represent mean ± SEM of at least 3 independent experiments.

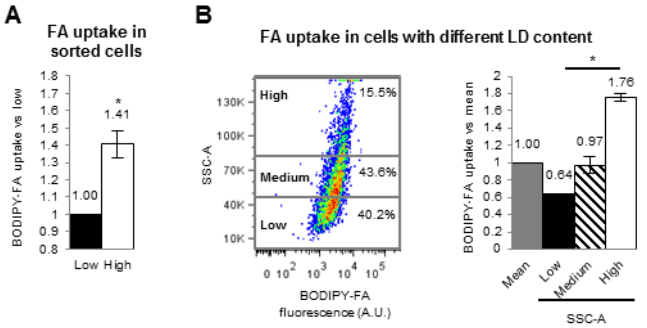

**Figure S4. (A)** Fluorescent thin-layer chromatography of BODIPY-FA alone (left) and cells loaded with BODIPY-FA for 16h (as in Figure 4E) with and without 10µM Triacsin C (TRC). **(B)** Confocal microscopy of cells treated as in A. **(C)** AML12 cells loaded with BODIPY-FA as in A were fractionated in sucrose density gradients. The low density fraction (#1) contains the LDs whereas other membranes, such as the endoplasmic reticulum, remain in intermediate fractions (#4). The graph represents the % of BODIPY-FA fluorescence of each fraction. **(D)** Western blots showing distribution of ADRP (LDs) and Sec61 (ER) in the sucrose density gradients. (n=3).

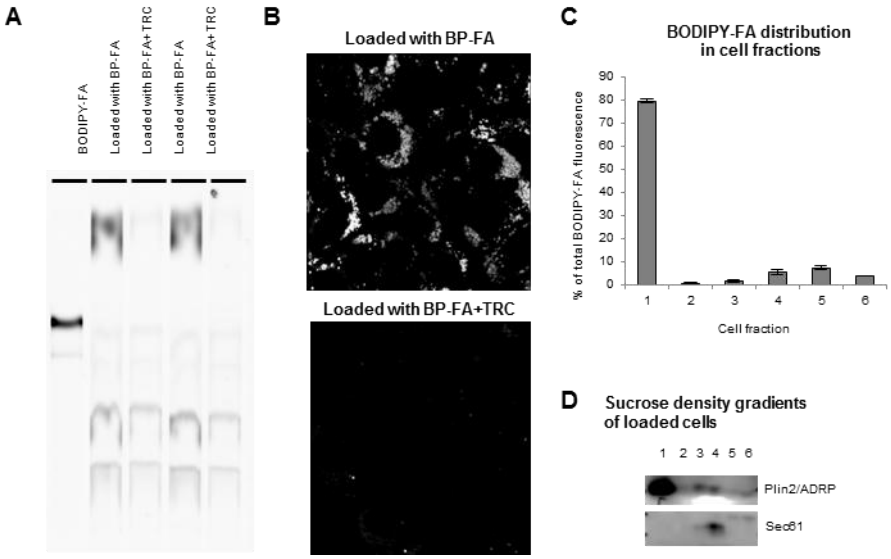

## Legends to supplementary movies.

(Movie S1 related to Figs.1E to 1GI) Liver was isolated as previously described [1], processed as detailed in Supplemental Methods and embedded tissues were imaged and sectioned in a 3View microscope at 3000X magnification and 2.25kV. 1000 consecutive sections covering an approximately 50 μm depth of the liver are shown.

(Movies S2 and S3 related to Figs.1E to 1GI) As an example of cell-to-cell heterogeneity image stacks of two adjacent cells selected from Movie S1 (related to Fig.1E, Cell 1 in Movie S2 and Cell2 in Movie S3) were processed for three-dimensional segmentation analysis in IMOD as described previously [2]. The translucent white lines indicate the plasma membrane, light blue lines the nuclei, and yellow lines the LDs. Volumetric data was extracted with the program IMODinfo and shown in Figs1H and 1I. See text for more details.

## Supplemental text.

**Validation of neutral lipid quantification by flow cytometry (supplemental text for Figure S1A).**

Nile red staining of neutral lipids was used to quantify LD levels. Nile Red discriminates triglycerides in LDs from triglycerides accumulated in the plasma membrane or the endoplasmic reticulum [3]. When Nile red-stained cells are examined at wavelengths of 580 nm or less, the fluorescence of the probe interacting with a highly hydrophobic environment such as LDs is maximized, whereas fluorescence corresponding to polar lipids from cellular membranes is minimized [4, 5]. Proportionality between Nile Red fluorescence and triglyceride content in form of LDs has been confirmed with NMR signals [6]. The relative increment measured with Nile Red and flow-cytometry was identical to the result obtained with an enzymatic method, or when alternative dyes such as BODIPY 493/503 were used (Fig S1A). The presence of Triacsin C, that inhibits the activation of FA to Acyl-CoA [7] , and thus incorporation into neutral lipids, highly reduced the levels of triglycerides quantified with the three methods.

**Causes of heterogeneity in LD content: extended explanation of the inhibitors used in Figures 2 and S3.**

To determine contributors to LD heterogeneity, we combined modification of environmental conditions with targeted impairment (Fig.2A). In principle, LD variability might simply reflect an asynchronous progression throughout the cell division cycle. However, when AML12 were FA-loaded and synchronized in $G_0$ by serum deprivation (Fig.S3G dark grey) or in the S phase with thymidine treatment (Fig.S3G light grey), they demonstrated identical heterogeneity as asynchronous cells (Figs.S3F), suggesting that cell cycle differences do not significantly affect LD loading neither promote heterogeneity.

Turnover of lipids leaving LDs is also a possible source of heterogeneity. Lipids in LDs are metabolized via lipases or autophagy (Fig.2A, red or purple arrow respectively). To test the contribution of each pathway, cells were now FA-loaded in the presence of DEUP or E600 (to inhibit lipases) or 3MA (to inhibit autophagy)[7-9]. Interestingly, DEUP increased the LD content by 50% and reduced the %rCV (Figs.2G and 2J), suggesting an active LD turnover and a significant cellular variability in the process. This was confirmed

by treating cells with the alternative lipase inhibitor E600 (FigS3A and S3B). In contrast, 3MA slightly decreased the LD levels and the %rCV, suggesting that upon these conditions LDs are not significantly metabolized by this mechanism but are supplied with lipids from autophagy.

De novo lipid synthesis (green arrow, Fig 2A) is an important source of lipids for lipid droplet biogenesis and a potential cause of heterogeneity. Then we analysed the effect of platensimycin, a specific inhibitor of lipogenesis [10], on LD accumulation. The treatment with platensimycin did not affect LD loading and heterogeneity, suggesting that lipogenesis do not contribute to generate LD heterogeneity.

In hepatocytes, lipids are metabolized into energy and lipid intermediates in mitochondria (orange arrow Fig.2A). To determine whether mitochondrial activity contributed to heterogeneity, cells were FAs-loaded in the presence of etomoxir, an inhibitor of the carnitine palmitoyltransferase 1 that mediates the uptake of FA by the mitochondria [11]. Interestingly, etomoxir increased the LD content and reduced the %rCV (Figs.2G and 2J). Thus, systems with reduced mitochondrial activity will experience both increased LD content and reduced heterogeneity.

Stochasticity is often caused by fluctuations at the level of transcription and translation. Cycloheximide blocks translational elongation and inhibits proteins synthesis. When cells were FA-loaded in the presence of cycloheximide, the %rCV was significantly reduced (Fig. 2J). Note that this block in protein synthesis has a moderate effect on LD accumulation (Figs.2G), demonstrating that the LD heterogeneity is not simply a passive marker of overall lipid levels as the etomoxir and cycloheximide-treated cells have very different LD levels, but almost the same heterogeneity.

We also evaluated heterogeneity sources during unloading: previously FA-loaded cells were incubated 16h in FA-free media in the presence of the inhibitors. Metabolization of LDs was reduced by inhibition of lipases (DEUP and E600), autophagy (3MA), beta-oxidation (etomoxir), and protein synthesis (cycloheximide)

(Fig.2H and S3C). In contrast to the loading case, 3MA clearly affected the LD content, suggesting that lipo-autophagy is active under this condition. As expected, inhibition of beta-oxidation (with etomoxir) and lipolysis (with DEUP or E600) reduced heterogeneity when compared to the cells unloaded without the inhibitors (Fig.2K and S3D). In contrast, cycloheximide and 3MA had no effect on the %rCV, suggesting that during unloading both mechanisms are activated proportionally to the LD content of each cell.

**Cell sorting by SSC-A (supplemental text for Figure 3).**

The use of the SSC-A as an equivalent to the LD content is not only demonstrated here but also by other authors [12, 13]. In our study, the SSC-A was not really used to calculate the LD content of the cells. The SSC-A was only used as an approximate criterion and a convenient tool during the experiments involving sorting of cells, to avoid any potential long term toxic effect of neutral lipid dyes when cells are cultured 7 days after sorting or interference with other dyes used to measure lipid uptake and ROS levels.

**High-lipid cells supply lipids to the population: accumulation of a fluorescent FA in LDs of high-lipid cells (Figure 4E).**

To test if high-lipid cells can supply stored lipids to the rest of cells, we accumulated a BODIPY-FA in the LDs of high-lipid cells (Fig.S5). Thus, cells were loaded for 24h with 175µg/ml FA and 1µM BODIPY-FLC16 was added only for the first 12h to allow cells to metabolize and incorporate the FA-BODIPY in LDs. Then, the distribution of BODIPY-tagged lipids into the different lipid species was analysed by thin layer chromatography. After loading, BODIPY-FA was metabolized as previously described [14], and this metabolization was inhibited by Triacsin C (Fig. S5A). Moreover, accumulation of the BODIPY-FA into LDs was confirmed by confocal microscopy (Fig S5B) and cell fractionation in sucrose density gradient (Fig. S5C). The BODIPY-FA fluorescence accumulated in the LD fraction identified by the presence of the LD marker Plin2/ADRP (Fig.S5D).

## Supplemental Methods.

**Reagents**

Nile red, BODIPY-FLC16, Hoechst-33258, Cell Trace™ Far Red DDAO-SE and BODIPY 493/503 were from Molecular Probes, Invitrogen. Fatty acid free BSA, collagenase type IV, 2',7'-Dichlorofluorescein diacetate ($H_2$DCFDA), palmitic acid, thymidine, diethylumbelliferyl phosphate (DEUP), 3-methyl-adenine (3MA), platensimycin (PTM), diethyl-*p*-nitrophenyl phosphate (E600), etomoxir (ETO) and cycloheximide (CHX) were purchased from Sigma-Aldrich (St. Louis, MO, USA). Triacsin C (TRC) was from Santa Cruz Biotechnology (California, USA). Oleic acid and mowiol were from Calbiochem (La Jolla, CA, USA).

**Cell culture and oleic acid treatment.**

AML12 (ATCC, CRL-2254) were cultured in 1:1 mixture of Dulbecco's modified Eagle's medium (DMEM, Biological Industries) and Ham's F12 medium with 0.005mg/ml insulin, 0.005mg/ml transferrin, 5ng/ml selenium, 40ng/ml dexamethasone (from Sigma-Aldrich's ITS Media Supplement) and 10% v/v Fetal Bovine Serum (FBS, Biological Industries). Vero, COS-1, HepG2, C2C12, HeLa, 3T3L1 and MEF cells were cultured in DMEM 10% v/v FBS. Mediums were supplemented with 4mM L-glutamine, 1mM pyruvate (Sigma-Aldrich, St. Louis, MO, USA) and with 50 U/ml Penicillin, 50µg/ml Streptomycin, and Non-Essential Amino Acid (Biological Industries). Oleic acid and/or Palmitic acid were conjugated to FA-free bovine serum albumin (BSA) at a molar ratio of 6:1 [7]. For LD loading, AML12 cells were plated at 40% confluence in 6-well plates and treated the next day during 24h with Oleic acid 175µg/ml (FA) unless it is specified and in some cases with the indicated drugs during the 24h treatment. For unloading experiments, cells were additionally incubated 16h in the medium described above but without serum (medium without FA), without serum and the indicated drugs, or with different oleic acid concentrations.

**Triglyceride measurement:**

Cells were washed twice with cold PBS before being scraped into ice-cold 10mM Tris, pH 7.5, 150mM NaCl, 5mM EDTA, and a mixture of protease inhibitors, and then disrupted by sonication. The triglyceride

measurement was performed with the Triglyceride assay kit (Wako Pure Chemicals, Osaka, Japan) following the manufacturer's instructions.

**Animals.**

C57BL/6 mice received care in compliance with the European Community. Food and water were available *ad libitum* except starved mice that were starved during 12h. Partial hepatectomy was carried out as previously described [1] and mice were collected 24 and 48h after. Animals were perfunded with 50ml of 2.5% glutaraldehyde/PBS and livers were extracted, fixed in 2.5% glutharaldehyde and 2% paraformaldehyde/PBS at 4ºC, embedded in Spurr (Sigma-Aldrich) and postfixed in $OsO_4$. Semi-thin sections of 1µm of thickness, performed in an Ultracut were stained with methylene-blue and images obtained in a Leica DMRB microscope with the 63x objective. Primary hepatocytes from 8–12 weeks old mice were isolated as previously [15] and cultured in DMEM:Hams (1:1) 10%FBS on glass coverslips coated with rat tail collagen.

**Fluorescence microscopy.**

All preparations were fixed 1h in 4% paraformaldehyde to preserve LD structure. Then in some cases cells were stained 10 min with 3µg/ml Hoechst in PBS. Nile red staining for microscopy was performed as previously [16]. Images corresponding to single confocal sections were taken in a Leica TCS SP5 laser scanning confocal spectral microscope, using 405nm laser for Hoechst detection and 514nm laser for Nile red detection; or in a Leica TCS SL laser scanning confocal microscope using 488nm laser for BODIPY-FLC16 detection and the 633nm laser for Cell Tracer DDAO-SE detection, in both cases with a 63x oil immersion objective lens with a numerical aperture (NA) of 1.4. and a pinhole of 1.5 A.U. Images were analysed using Adobe Photoshop CS software (Adobe Systems Inc) and Image J (NIH).

**3View electron microscopy.**

Liver tissue was isolated as previously described [1]. Tissue was fixed in 2.5% glutaraldehyde, washed in PBS and postfixed in 2% OsO4 with 1.5% potassium ferricyanide. Samples were washed in water, incubated in a

1% (w/v) thiocarbohydrazide solution for 20min. Liver tissue was postfixed again in 2% OsO4, washed (H2O) and stained with 1% uranyl acetate. Tissues was further stained with a lead aspirate solution (20mM lead nitrate, 30mM asparatic acid, pH 5.5), serially dehydrated in acetone, infiltrated with durcupan resin and polymerised. Embedded tissues were imaged and sectioned in a 3View microscope at 3000X magnification and 2.25kV. Image stacks were processed for three-dimensional segmentation analysis in IMOD as described previously [2]. Volumetric data was extracted with the program IMODinfo.

**Flow cytometry.**

To analyse the LD content, cells were trypsinized, washed in PBS and stained for 15 min in 5µg/ml Nile red in PBS or 1µg/ml BODIPY-493/503 in PBS. For ROS quantification, cells were plated in 6-well plates at 40% confluence and the next day loaded 24h with 175µg/ml FA. Then, cells were incubated 10 min with 15µM $H_2$DCFDA in phenol-free DMEM (Sigma-aldrich) without serum, trypsinized and resuspended in PBS. For the FA uptake assay cells were incubated with BODIPY®FLC16 at 1µM during 10min in their culture medium and then harvested by tripsinization and ressuspended in PBS. For cell cycle analysis cells were harvested, fixed overnight at 4ºC in ethanol 70% and stained with 30µg/ml Hoechst in PBS.

For the experiments with mixed cell populations, non-loaded cells were tripsinized and stained with 0,5µM Cell Trace DDAO-SE in PBS for 5min shacking at room temperature and then co-cultured with the indicated populations. LD content was analysed by BODIPY 493/503 staining and ROS was quantified by $H_2$DCFDA as described above. For the FA uptake assay cells were incubated 10 min with 1µM BODIPY-FLC16, trypsinized and resuspended in PBS. For the FA exchange assay, BODIPY-FLC16 was incorporated into LDs treating cells 12h with 175µg/ml FA and 1µM BODIPY-FLC16 and additionally 12h with 175µg/ml FA. Then cells were trypsinized and mixed 1:1 with non-loaded cells labelled with Cell Trace DDAO-SE.

Cells were analysed using FACS Canto II, with the violet laser (405nm) as the excitation source and collecting the fluorescence with the 450/50 filter (Hoechst); the blue laser (488nm) and collecting the fluorescence

with the 585/42 (NR), 530/30 (BODIPY-FLC16, BODIPY 493/503 and $H_2$DCFDA) filters or the 633nm laser and collecting the fluorescence with 660/20 filter (DDAO-SE ) filters. Data was analysed with the CellQuest software (Becton & Dickinson) and FlowJo software (TreeStar).

**Cell sorting.**

AML12 ($3x10^4$ /$cm^2$) were treated 24h with 175μg/ml FA. Cells were trypsinized and resuspended in PBS, 1% v/v FBS, 1mM EDTA, and 25mM Hepes pH 7.0. Then cell density was adjusted to $7x10^6$ cells/ml and cells were filtered with a cell-strainer of 35μm (Becton & Dickinson) and sorted by SSC-A value in a BD FACS Aria SORP with the 488nm Laser at 20mWatt, collecting the 15% of the population in the extremes. The efficiency of the SSC-A as the sorting criteria was always confirmed after every sorting by staining some of the cells with 5μg/ml Nile Red (see above). ROS levels were quantified incubating cells with 15μM $H_2$DCFDA/PBS for 10 min, cells were then washed in PBS and cellular fluoresce was analysed by flow-cytometry. Fatty acid uptake was quantified incubating cells in 1μM BODIPY®FLC16/PBS for 10min, cells were then washed in PBS, and cellular fluoresce was analysed by flow-cytometry. In parallel, cells ($2.5x10^4$ cells/$cm^2$) were plated 7 days in normal medium, additionally treated 24h with 175μg/ml FA and LD content was analyzed by flow cytometry as described above.

**Cell fractionation.**

Cells were incubated 12h with 175μg/ml oleic acid and 1μM BODIPY-FLC16 and additionally 12h with 175μg/ml FA. Cell fractionation and western blot were performed as previously [16]. The fluorescence of each fraction was measured in a fluorescence plate reader (Synergy2 BioTek).

**Fluorescent thin layer chromatography.**

Cells treated with OA and BODIPY-FLC16 were tripsinized and total lipids were extracted as described previously [17]. The organic phase was collected, dried, resuspended with chloroform and spotted onto 60Å silica gel TLC plates (Whatmann, Partisil® LK6D), and dried for several minutes. A solvent system of

hexane/diethyl ether/acetic acid (70:30:1) was added to TLC chamber and allowed to equilibrate and plates were run until the solvent front reached 1cm from the top of the plate. After drying, plates were scanned (ImageQuantT™LAS4000 biomolecular imager, GE Healthcare Bio-sciences AB, Sweden) using the blue fluorescence light (excitation: 460nm; emission: Y515Di filter) to detect fluorescent bands.

**Statistical analysis.**

All data shown in graphs are the mean and SEM, and the statistical significance were determined using the Student's t test (*P<0.05; **P<0.01; ***P<0.001).

## Supplemental References.


1. Fernandez, M.A., Albor, C., Ingelmo-Torres, M., Nixon, S.J., Ferguson, C., Kurzchalia, T., Tebar, F., Enrich, C., Parton, R.G., and Pol, A. (2006). Caveolin-1 is essential for liver regeneration. Science *313*, 1628-1632.
2. Noske, A.B., Costin, A.J., Morgan, G.P., and Marsh, B.J. (2008). Expedited approaches to whole cell electron tomography and organelle mark-up in situ in high-pressure frozen pancreatic islets. J Struct Biol *161*, 298-313.
3. Gubern, A., Casas, J., Barcelo-Torns, M., Barneda, D., de la Rosa, X., Masgrau, R., Picatoste, F., Balsinde, J., Balboa, M.A., and Claro, E. (2008). Group IVA phospholipase A2 is necessary for the biogenesis of lipid droplets. J Biol Chem *283*, 27369-27382.
4. Greenspan, P., Mayer, E.P., and Fowler, S.D. (1985). Nile red: a selective fluorescent stain for intracellular lipid droplets. J Cell Biol *100*, 965-973.
5. Greenspan, P., and Fowler, S.D. (1985). Spectrofluorometric studies of the lipid probe, nile red. J Lipid Res *26*, 781-789.
6. Al-Saffar, N.M., Titley, J.C., Robertson, D., Clarke, P.A., Jackson, L.E., Leach, M.O., and Ronen, S.M. (2002). Apoptosis is associated with triacylglycerol accumulation in Jurkat T-cells. Br J Cancer *86*, 963-970.
7. Brasaemle, D.L., Rubin, B., Harten, I.A., Gruia-Gray, J., Kimmel, A.R., and Londos, C. (2000). Perilipin A increases triacylglycerol storage by decreasing the rate of triacylglycerol hydrolysis. J Biol Chem *275*, 38486-38493.
8. Ouimet, M., Franklin, V., Mak, E., Liao, X., Tabas, I., and Marcel, Y.L. (2011). Autophagy regulates cholesterol efflux from macrophage foam cells via lysosomal acid lipase. Cell Metab *13*, 655-667.

9. Singh, R., Kaushik, S., Wang, Y., Xiang, Y., Novak, I., Komatsu, M., Tanaka, K., Cuervo, A.M., and Czaja, M.J. (2009). Autophagy regulates lipid metabolism. Nature *458*, 1131-1135.

10. Wu, M., Singh, S.B., Wang, J., Chung, C.C., Salituro, G., Karanam, B.V., Lee, S.H., Powles, M., Ellsworth, K.P., Lassman, M.E., et al. (2011). Antidiabetic and antisteatotic effects of the selective fatty acid synthase (FAS) inhibitor platensimycin in mouse models of diabetes. Proc Natl Acad Sci U S A *108*, 5378-5383.

11. Koves, T.R., Ussher, J.R., Noland, R.C., Slentz, D., Mosedale, M., Ilkayeva, O., Bain, J., Stevens, R., Dyck, J.R., Newgard, C.B., et al. (2008). Mitochondrial overload and incomplete fatty acid oxidation contribute to skeletal muscle insulin resistance. Cell Metab *7*, 45-56.

12. Lee, Y.H., Chen, S.Y., Wiesner, R.J., and Huang, Y.F. (2004). Simple flow cytometric method used to assess lipid accumulation in fat cells. J Lipid Res *45*, 1162-1167.

13. Aldridge, A., Kouroupis, D., Churchman, S., English, A., Ingham, E., and Jones, E. (2013). Assay validation for the assessment of adipogenesis of multipotential stromal cells-a direct comparison of four different methods. Cytotherapy *15*, 89-101.

14. Carten, J.D., Bradford, M.K., and Farber, S.A. Visualizing digestive organ morphology and function using differential fatty acid metabolism in live zebrafish. Dev Biol *360*, 276-285.

15. Bosch, M., Mari, M., Herms, A., Fernandez, A., Fajardo, A., Kassan, A., Giralt, A., Colell, A., Balgoma, D., Barbero, E., et al. (2011). Caveolin-1 deficiency causes cholesterol-dependent mitochondrial dysfunction and apoptotic susceptibility. Curr Biol *21*, 681-686.

16. Ingelmo-Torres, M., Gonzalez-Moreno, E., Kassan, A., Hanzal-Bayer, M., Tebar, F., Herms, A., Grewal, T., Hancock, J.F., Enrich, C., Bosch, M., et al. (2009). Hydrophobic and basic domains target proteins to lipid droplets. Traffic *10*, 1785-1801.

17. Bligh, E.G., and Dyer, W.J. (1959). A rapid method of total lipid extraction and purification. Can J Biochem Physiol *37*, 911-917.